*Korean J. Chem. Eng.*, **25**(5), 1054-1059 (2008)

# Autothermal reforming of methane to syngas with palladium catalysts and an electric metal monolith heater

**Kyoungmo Koo*, Jaekyung Yoon**, Changha Lee*, and Hyunku Joo**,†**

*Chemical Eng. Dept., Yonsei University, 134 Sinchon-dong, Seodaemun-gu, Seoul 120-749, Korea
**Climate Change Technology Division, Korea Institute of Energy Research,
71-2 Jang-dong, Yuseong-gu, Daejeon 305-343, Korea
(*Received 21 March 2008 • accepted 8 July 2008*)

**Abstract**−The autothermal reforming of methane to syngas for use in the Fischer-Tropsch synthesis was studied in this work over PdO containing various combinations of $CeO_2$, BaO or SrO in a washcoated form on a metallic monolith at atmospheric pressure. This study focused on the autothermal operation of the system, in which an electric heater inside the reactor was used only to reach the ignition temperature, and thereafter the autothermal reaction successfully sustained itself without any external heat source. It was concluded from the experiments that the $PdO/Al_2O_3$ catalyst was better than the others, except for $PdO\text{-}CeO_2\text{-}BaO\text{-}SrO/Al_2O_3$, which showed similar performance in terms of the $CH_4$ conversion and $H_2$+CO selectivity, while affording a higher $H_2$/CO ratio (close to ca. 3) than the $PdO/Al_2O_3$ catalyst did (close to ca. 2). The gas hourly space velocity and $O_2/CH_4$ ratio governed the methane conversion, while the $H_2O/CH_4$ ratio controlled the $H_2$/CO ratio. A methane conversion of ~87%, $H_2$+CO selectivity of ~94%, $H_2$/CO ratio of ≤2.9, and M factor ≅2.15 were obtained under the conditions of a gas hourly space velocity (GHSV) of 120,000 $h^{-1}$, $O_2/CH_4$=0.6 and $H_2O/CH_4$=0.5.

Key words: Autothermal Reforming, Palladium, Syngas, F-T Synthesis, $H_2$/CO Ratio

## INTRODUCTION

Recently, due to the increased interest in clean synfuels caused by the stringent environmental regulations, gas-to-liquid (GTL) technology has had a great deal of publicity. The expectation of the possible advent of peak oil has also led many researchers to become interested in GTL technology. The production of syngas is of great importance in the GTL process, because syngas is the feedstock for the Fischer-Tropsch synthesis and syngas manufacture is responsible for ca. 60% of the investment in GTL plants. One of the resources for syngas production is natural gas, which consists of 80-90% methane, but which is sometimes found in remote locations and in uneconomical amounts. Hence, technologies to achieve energy-saving efficiency and compact design must be adopted in this process. Currently, catalytic partial oxidation (CPOx) and autothermal reforming (ATR) have been the preferred technology due to their high methane conversion and syngas yields with millisecond contact times and ability to be conducted in comparably small reactors ideal for decentralized applications [1], as described in a previous study in which the authors described the reaction mechanism on the basis of the species and temperature profiles with a spatial resolution of about 300 μm, comparing Rh and Pt as catalysts for the CPOx reaction. The proposed mechanism of the methane CPOx reaction, which is still open to question, consists of direct (Eq. (1)) and indirect (Eqs. (2)-(4)) mechanisms as follows.

$$CH_4+(2-x/2-y/2)O_2 \rightarrow xH_2+yCO+(2-x)H_2O+(1-y)CO_2,\ 0\le x\le 2,\ 0\le y\le 1 \quad (1)$$

$$CH_4+2O_2 \rightarrow CO_2+2H_2O,\ \Delta H_r^o=-803\ \text{kJ mol}^{-1} \quad (2)$$

$$CH_4+H_2O \rightarrow CO+3H_2,\ \Delta H_r^o=+206\ \text{kJ mol}^{-1} \quad (3)$$

$$CH_4+CO_2 \rightarrow 2CO+2H_2,\ \Delta H_r^o=+247\ \text{kJ mol}^{-1} \quad (4)$$

The direct mechanism assumes that $H_2$ and CO are the primary reaction products formed by partial oxidation (Eq. (5)) in the presence of gas-phase $O_2$ including the competitive formation of $H_2O$ and $CO_2$.

$$CH_4+0.5O_2 \rightarrow CO+2H_2,\ \Delta H_r^o=-36\ \text{kJ mol}^{-1} \quad (5)$$

The indirect mechanism postulates a two-zone design, one of which is the strongly exothermic combustion of $CH_4$ at the entrance of the catalyst layer and the other of which is the subsequent, strongly endothermic steam- and/or $CO_2$-reforming process. Various catalysts on different supports have been reported to be active for the methane CPOx reaction, most of which contain a group VIII metal as their active component (e.g. Rh, Pt, Ru, Ni) on an oxide support [2,3]. The use of monolithic catalysts serves to minimize the pressure drop along the reactor and to lessen the hot spot temperatures [4].

In this study, the autothermal reforming of methane was investigated in order to produce syngas with the optimal ratio of $H_2$ to CO (≈2) for the Fischer-Tropsch process. Palladium with or without various promoters such as $CeO_2$, BaO and SrO was selected and compared, instead of nickel and rhodium which have previously been studied [3-10]. The catalysts were prepared in the metal monolith-washcoated form in order to enhance their activities at high gas flow rates.

## EXPERIMENTAL

### 1. Experimental Setup and Calculation

The ATR reaction operated at atmospheric pressure was carried out in a stainless-steel reactor (inside diameter of 5 cm) in which

†To whom correspondence should be addressed.
E-mail: hkjoo@kier.re.kr

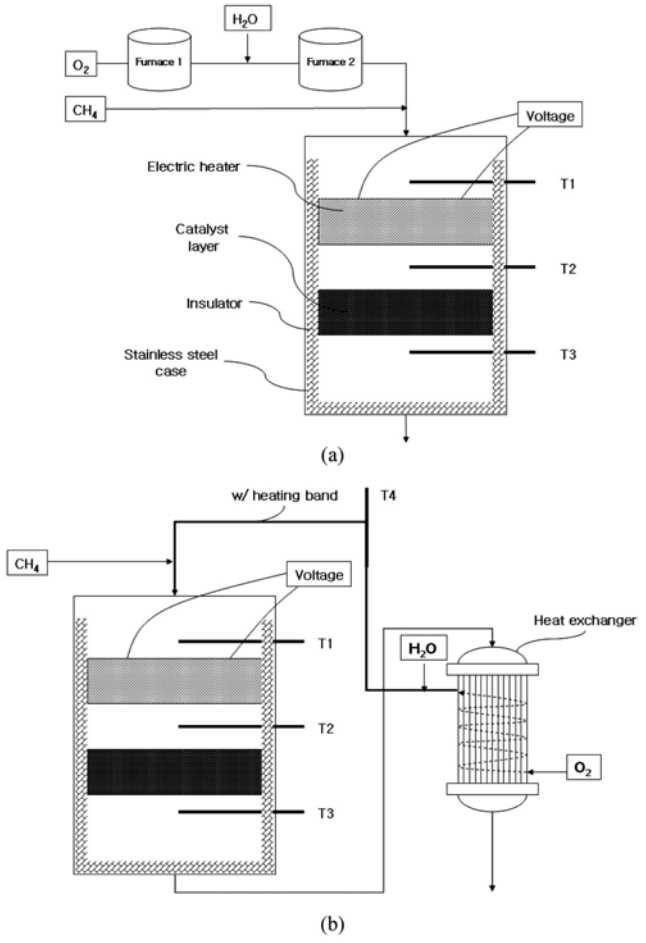


**Fig. 1. Schematic diagrams of the autothermal reforming system with an electric heater: (a) with furnaces, (b) with a heat exchanger.**

an insulator (thickness: 0.5 cm) and cylindrical metallic monolith catalysts (volume: ca. 25 $cm^3$, diameter: 4 cm, height: 2 cm) were located. Fig. 1 shows a schematic view of the ATR reactor and the stream of the reactants with either two furnaces or a heat exchanger. An electric heater (EH), placed in front of the washcoated monolith catalyst layer, ensured the even distribution of the reactant gases, due to the form of the monolith, and provided the necessary heat to preheat the catalyst layer to the catalytic ignition temperature of the feed mixture (approximately 450 °C), in order to initiate the partial oxidation of methane [11]. Water was fed by an HPLC pump (Series II, LabAlliance, USA) to a line leading to the furnace or heat exchanger. Hence, steam was supplied to the reactor through either the furnaces at 400 °C (Fig. 1(a)) or the heat exchanger (Fig. 1(b)). Thermocouples were placed within the reactor to record the temperature profile along the reactor axis and at the pre-heated output stream of oxygen-water mixture from the heat exchanger when used. The thermocouples placed inside the reactor were in thermal contact with the gases, but not with the catalyst layer; therefore, all of the temperature profiles recorded by the thermocouples are the gas temperatures. The hot product gas was cooled at the condenser and the remaining steam was again screened by a moisture trap placed before the sampling port. The volumetric flow rate of the gas mixture was measured by a dry gas meter (DS-16A-T, SHINAGAWA, Japan), while the compositions of the dry product gases were analyzed by a gas chromatograph (HP5890, TCD) equipped with a column (CARBOSPHERE80/100, Alltech, USA) and on-line gas analyzer (PG-250, HORIBA, Japan). Based on the compositions and molar flow rate of the product gases, the conversion of $CH_4$, the selectivity to $H_2$ plus CO, and the ratio of $H_2$ to CO were calculated, in order to investigate the influence of the O/C and steam/C ratios, as well as the space velocity (Eqs. (6)-(8)). In addition, the module M in Eq. (9), by which a stoichiometric match between the syngas produced and the final product is established for the GTL applications which convert both CO and $CO_2$ into liquid hydrocarbons, was identified. For the production of Fischer-Tropsch liquids in the diesel range, M should have a value of 2.1 [11,12].

$$CH_4 \text{ conv. } (\%) = \text{flow rate of } (CO+CO_2) \times 100 \,/\text{flow rate of } (CH_4+CO+CO_2) \quad (6)$$

$$H_2+CO \text{ selectivity } (\%) = \text{flow rate of } (H_2+CO) \times 100 \,/\text{flow rate of } (H_2+CO+CO_2) \quad (7)$$

$$H_2/CO \text{ ratio} = \text{flow rate of } H_2 / \text{flow rate of CO} \quad (8)$$

$$M = (H_2 - CO_2)/(CO_2+CO) \quad (9)$$

## 2. Preparation of Catalyst

In the studies by Bhattachary et al. [9] and Mouaddib et al. [13], PdO catalysts on various support materials were reported to be active for the partial oxidation of methane and steam reforming of methane. By contrast, Torniainen et al. [14] reported that a PdO catalyst displayed only moderate activity for the partial oxidation of methane (POx) and became deactivated due to coke formation. Thus, in our group, various combinations of the PdO catalyst with BaO, SrO and $CeO_2$ were considered to investigate the autothermal performance. The selected relative composition of the components by weight was PdO(2)/$CeO_2$(23)/BaO(11)/SrO(0.8)/$Al_2O_3$ and, hence, this composition was used for the preparation of the catalyst. Promoted alumina was prepared by the wet impregnation method. Fine particles of $\gamma$-$Al_2O_3$ (Aldrich, 198 $m^2/g$) were made into a slurry with an aqueous solution of $(C_2H_3O_2)_2Ba$ (Aldrich), $(C_2H_3O_2)_3Ce{\cdot}xH_2O$ (Aldrich), and $(C_2H_3O_2)_2Sr$ (Aldrich) at 50 °C for 12 hours. The suspension was filtered and dried in air at 120 °C for 3 hours. The dried sample was heated and then calcined at temperatures ranging from 600 to 900 °C for 3 hours. The calcined samples were crushed to fine particles (less than 40 mesh) with a ball-mill. A highly concentrated slurry of fine particles of the promoted alumina and palladium nitrate solution ($Pd(NO_3)_2$) was prepared for the purpose of washcoating the monolith. The washcoated metallic monoliths were calcined at 900 °C for 8.5 hours in air. The amount of the washcoated catalyst was 0.21 g/$cm^3$ of the monolith. The detailed procedures used for the preparation of the metallic monolith are described in another work [15]. The detailed characterization of the prepared catalysts is beyond the scope of this article. However, the surface areas of the catalysts were characterized by the multi-point BET method using a BEL-SORP-MINI (BEL-CAT, Japan), temperature-programmed reduction (TPR) by $H_2$ and metal dispersion by CO gas (BEL-CAT, Japan), and the components phases were characterized by powder XRD using CuK$\alpha$ radiation (Miniflex, Rigaku, Japan).

**Table 1. BET analysis of the prepared catalysts (averaged pore diameter is 2 nm for all species)**

| | PdO | PdO+Ce | PdO+Ba | PdO+Sr | PdO+Ce+Ba | PdO+Ba+Sr | PdO+Ce+Sr | PdO+Ce+Ba+Sr |
|---|---|---|---|---|---|---|---|---|
| BET ($m^2\ g^{-1}$) | 94.33 | 41.43 | 54.96 | 68.58 | 51.94 | 67.78 | 60.61 | 33.039 |
| Pore volume ($cm^3\ g^{-1}$) | 0.0465 | 0.0205 | 0.0272 | 0.0338 | 0.0258 | 0.0337 | 0.0300 | 0.0164 |

## RESULTS AND DISCUSSION

### 1. Characterization of the Catalysts

The surface area of the prepared catalysts was high for $PdO/Al_2O_3$ (94.3 $m^2/g$) and low for $PdO/CeO_2/BaO/SrO/Al_2O_3$ (33 $m^2/g$) and those of the others are shown in Table 1. The pore volumes for the catalysts ranged from 0.0164 to 0.0465 $cm^3/g$. The pore volume was linearly correlated with the surface area. The dispersion of the Pd particles was measured through the pulse injection method with 99.9% CO carried by helium, where the metal dispersions were 5.6± 0.2% and 17.3±0.1% for $PdO/Al_2O_3$ and $PdO/CeO_2/BaO/SrO/Al_2O_3$, respectively.

The broader XRD peaks (empty squares at $2\theta$=33.8, 60.7 and 71.2) for PdO as well as for the other components provided evidence of their good dispersion on the promoted supports (Fig. 2). The difference in the concentration of the components was clearly reflected in their characteristic peak intensities and sharpnesses. The curves for the temperature-programmed reduction by $H_2$ of the used catalysts from 30° to 950 °C at 5 °C/min were obtained and no noticeable relation between the activity and the TPR results was observed. The results obtained from this study showed that the $PdO/Al_2O_3$ catalyst was better than the others except for $PdO\text{-}CeO_2\text{-}BaO\text{-}SrO/Al_2O_3$, which showed similar performance in terms of the $CH_4$ conversion and $H_2$+CO selectivity, while providing a higher $H_2$/CO ratio (close to ca. 3) than $PdO/Al_2O_3$ did (close to ca. 2). Fig. 3 shows a comparison of the activities of the prepared catalysts in terms of the methane conversion and $H_2$/CO ratio under the given conditions ($5 \le CH_4$ (L/min)$\le 10$, $0.5 \le O_2/CH_4 \le 0.55$, $0.6 \le H_2O/CH_4 \le 1$, catalyst volume=25 $cm^3$). The Ba-containing catalysts without Ce and Sr were not active in the ATR reaction, while the catalysts without Ba showed much higher $H_2$/CO ratios than the others except for $PdO/Al_2O_3$. The promotional effect of the promoters in this study seemed clear only when they were used simultaneously. As a result, the ATR activity was in the order of $PdO/CeO/BaO/Al_2O_3$, $PdO/SrO/BaO/Al_2O_3 << PdO/BaO/Al_2O_3 < PdO/CeO_2/SrO/Al_2O_3 < PdO/SrO/Al_2O_3 < PdO/CeO_2/Al_2O_3 < PdO/Al_2O_3 \le PdO/BaO/CeO_2/SrO/Al_2O_3$. From this point on, $PdO/Al_2O_3$ was selected for further investigation. With the $PdO/Al_2O_3$ catalyst, a methane conversion of ~87%, $H_2$+CO selectivity of ~94%, $H_2$/CO ratio ≅2.9, and M factor ≅2.15 were obtained under the conditions of a gas hourly space velocity (GHSV) of 120,000 $h^{-1}$, $O_2/CH_4$=0.6 and $H_2O/CH_4$=0.5.

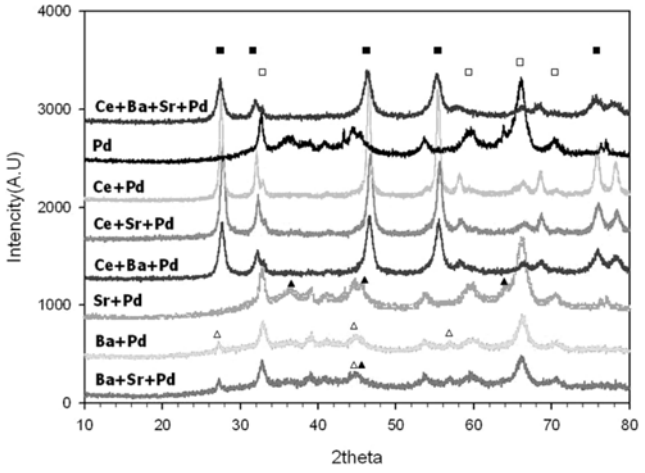


**Fig. 2. XRD spectra of the used catalysts (■: CeO, □: PdO, ▲; SrO, △: BaO).**

### 2. Start-up Stability

Several time-course temperature profiles at the beginning stage of the ATR reactions were selected and shown in Fig. 4, in which consistent start-up trends are clearly demonstrated with good repro-

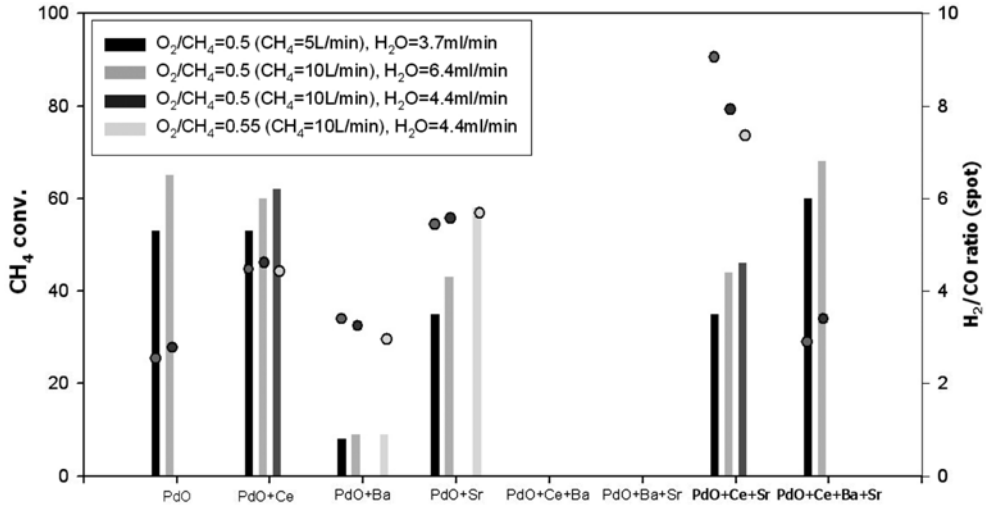


**Fig. 3. Comparison of the methane conversion and the ratio of $H_2$/CO.**

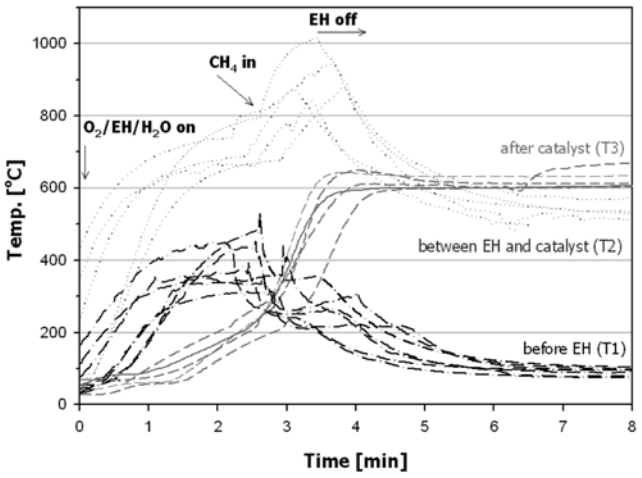


**Fig. 4. Time-course temperature profiles within the ATR reactors in Fig. 1 at the initial stage.**

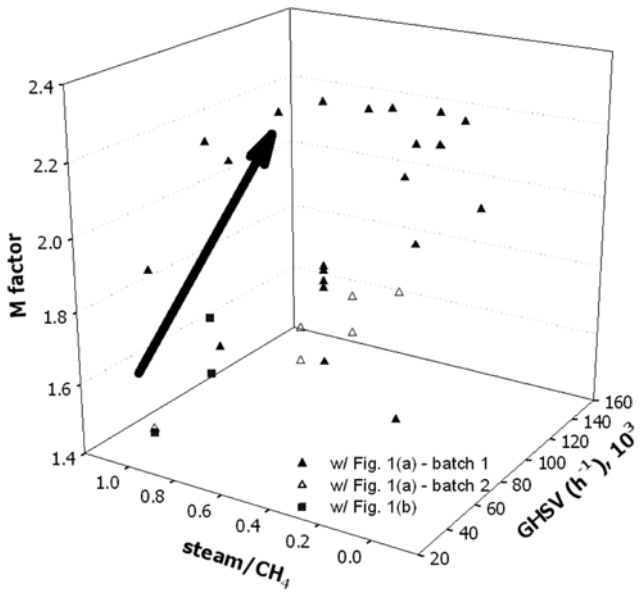


**Fig. 5. M factor (of the product obtained) from the autothermal reactions with the systems in Fig. 1 [data from Table 1-4, 5≤$CH_4$ (L/min)≤20, 2.5≤$O_2$ (L/min)≤10, 3.7≤$H_2O$ (mL/min)≤14.7, catalyst volume=25 $cm^3$].**

ducibility. Once the EH was switched on and $O_2$ and $H_2O$ allowed to flow, the temperature, T2, at the bottom of the EH abruptly increased up to 800 °C and then remained constant, while T1 at the top of the EH gradually increased to 400 °C and T3 at the bottom of the PdO-washcoated metallic monolith catalyst increased slowly to 200 °C within 3 min. The time of the methane injection turned out to be critical for the start-up of the system, because we observed that the POx reaction was initiated when the temperature, T3, was above 200 °C. This ignition temperature appears to depend on the activity of the catalyst, with the POx reaction starting at lower temperatures. Once methane was injected, T1 decreased due to its being injected at room temperature, while both T2 and T3 were increased by the methane oxidation reaction in the corresponding zones. At this point, when the exothermic reaction was initiated (after ca. 4 min), the EH was no longer of use and was turned off. The EH used up only 0.015 kWh during the initial stage of the ATR reaction and the ATR reaction sustained itself without any energy input under the given conditions. The time-course temperature profiles of T4, which, when this thermocouple was used, was placed between the inlet part of the reactor and the preheated cold stream from the heat exchanger, showed a steady increase in temperature to reach 100 °C about an hour after the initiation. Neither the furnaces nor the heat exchanger caused a decrease in the temperature, T2. A decrease in T2 would be followed by a decrease in the methane conversion and T3, because the reaction could not be sustained if a lower thermal input power were applied.

### 3. Influence of the Space Velocity, the O/C Ratio, and the Steam/C Ratio

A gas mixture of $CH_4$, $O_2$ ($0.5 \le O_2/CH_4 \le 0.67$ molar ratio) and $H_2O$ ($H_2O/CH_4 \le 1.0$) was passed through the reaction system at a gas hourly space velocity (GHSV) of up to 144,000 $h^{-1}$, as shown in either Fig. 1(a) with the furnaces or Fig. 1(b) with the heat exchanger. The GHSV was defined as the ratio of the product gas flow rate at 25 °C and 1 atm to the total volume of the catalyst. For example, if 5 L/min (300 L/hr) of $CH_4$ produce 15 L/min (900 L/hr) of $H_2$+CO with 25 $cm^3$ of catalyst layer, GHSV can be 36,000 $hr^{-1}$ (=900 L/hr/($25\times10^{-3}$ L)). The self-sustaining behavior of the reaction system mentioned above might be partly due to the high heat transfer ability of the metallic monolith, which is important in designing a compact reformer, because it allows high space velocities to be endured. Generally speaking, the M factor increased from ca. 1.46 at 36,000 $h^{-1}$ to 2.25 at 120,000-144,000 $h^{-1}$ as shown in Fig. 5 and Table 2. At higher space velocities, the greater heat release heats the catalyst layer, resulting in a higher reaction temperature and in-

**Table 2. Selected results from the autothermal reactions with the system in Fig. 1(a) [5≤$CH_4$ (L/min)≤20, 2.5≤$O_2$ (L/min)≤10, 3.7≤$H_2O$ (mL/min)≤8.9, catalyst volume=25 $cm^3$]**

| $CH_4$ (L/min) | GHSV ($hr^{-1}$) | $O_2/CH_4$ | $H_2O/CH_4$ | $CH_4$ conv. (%) | $H_2$+CO (%) | $H_2$/CO | Composition (%) | | | | |
|---|---|---|---|---|---|---|---|---|---|---|---|
| | | | | | | | $H_2$ | $O_2$ | CO | $CO_2$ | $CH_4$ |
| 5 | 36,000 | 0.5 | 1.0 | 54 | 88.0 | 2.6 | 48.3 | 1.1 | 18.7 | 8.5 | 23.6 |
| 10 | 72,000 | 0.5 | 0.6 | 74 | 89.0 | 2.89 | 59.1 | 0 | 20.5 | 9.8 | 10.5 |
| | | | | 65 | 93.3 | 2.38 | 55.6 | 0 | 23.3 | 5.7 | 15.4 |
| 15 | 108,000 | 0.5 | 0.6 | 76 | 96.0 | 2.07 | 58.3 | 0 | 28.2 | 3.6 | 9.9 |
| | | | | 69 | 94.0 | 2.10 | 55.0 | 0 | 26.3 | 4.8 | 13.9 |
| 20 | 144,000 | 0.5 | 0.6 | 70 | 95.0 | 2.11 | 55.6 | 0 | 26.4 | 4.6 | 13.5 |

**Table 3. Selected results on the effect of steam/$CH_4$ ratio from the autothermal reactions with the system in Fig. 1(a) [$CH_4$ (L/min)=7.5, $O_2$ (L/min)=10.2, 2.5≤$H_2O$ (mL/min)≤12.6, catalyst volume=25 $cm^3$]**

| $CH_4$ (L/min) | GHSV ($hr^{-1}$) | $O_2/CH_4$ | $H_2O/CH_4$ | T3 (°C, after catalyst layer) | $CH_4$ conv. (%) | $H_2$+CO (%) | $H_2$/CO |
|---|---|---|---|---|---|---|---|
| 17 | 120,000 | 0.6 | 1.0 | 750 | 80 | 92 | 3.3 |
| | | | 0.8 | 759 | 84 | 92 | 3.2 |
| | | | 0.6 | 771 | 86 | 94 | 3.1 |
| | | | 0.5 | 781 | 87 | 94 | 2.9 |
| | | | 0.4 | 790 | 87 | 95 | 2.9 |
| | | | 0.3 | 805 | 88 | 95 | 2.8 |
| | | | 0.2 | 815 | 88 | 96 | 2.7 |

**Table 4. Selected results on the effect of $O_2/CH_4$ ratio from the autothermal reactions with the system in Fig. 1(a) [7.5≤$CH_4$ (L/min)≤8.5, $O_2$ (L/min)=5, 2.7≤$H_2O$ (mL/min)≤3.1, catalyst volume=25 $cm^3$]**

| $CH_4$ (L/min) | GHSV ($hr^{-1}$) | $O_2/CH_4$ | $H_2O/CH_4$ | T3 (°C, after catalyst layer) | $CH_4$ conv. (%) | $H_2$+CO (%) | $H_2$/CO |
|---|---|---|---|---|---|---|---|
| 8.5 | | 0.59 | | 712 | 78 | 92 | 2.75 |
| 8.0 | ca. 72,000 | 0.63 | 0.5 | 750 | 84 | 92 | 2.63 |
| 7.5 | | 0.66 | | 800 | 89 | 92 | 2.80 |

**Table 5. Selected results from the autothermal reactions with the system in Fig. 1(b) [5≤$CH_4$ (L/min)≤7.5, 2.5≤$O_2$ (L/min)≤3.8, 3.7≤$H_2O$ (mL/min)≤5.6, catalyst volume=25 $cm^3$]**

| $CH_4$ (L/min) | GHSV ($hr^{-1}$) | $O_2/CH_4$ | $H_2O/CH_4$ | $CH_4$ conv. (%) | $H_2$+CO (%) | $H_2$/CO | Composition (%) | | | | |
|---|---|---|---|---|---|---|---|---|---|---|---|
| | | | | | | | $H_2$ | $O_2$ | CO | $CO_2$ | $CH_4$ |
| 5 | 36,000 | 0.5 | 1.0 | 60.2 | 88.8 | 2.53 | 50.1 | 2.5 | 19.8 | 8.7 | 18.9 |
| | | | | 62.0 | 90.6 | 2.41 | 52.6 | 0.0 | 21.8 | 7.7 | 17.9 |
| 7.5 | 72,000 | 0.5 | 1.0 | 67.9 | 92.9 | 2.38 | 56.2 | 0 | 23.6 | 6.1 | 14.0 |

creasing the M factor. In contrast, the effect of the amount of steam seemed negligible in the range used.

Selected results for the methane conversion, $H_2$+CO selectivity and $H_2$/CO ratio are shown in Table 2-Table 4 for the system with the furnaces and in Table 5 for the system with the heat exchanger.

At a GHSV of 120,000 $hr^{-1}$ with $O_2/CH_4$=0.6, a decrease in the steam/$CH_4$ ratio increased the reactor outlet temperature (T3), resulting in an increase in the methane conversion and $H_2$+CO selectivity and a decrease in the $H_2$/CO ratio (Table 3). According to the data on the compositions of the products at each sampling time, the amounts of $CH_4$ and $CO_2$ steadily decreased as the proportion of CO increased and that of $H_2$ decreased. This could be explained by the reverse water gas shift reaction. The effect of the O/C ratio is shown in Table 4, where an increase of the methane conversion with increasing reactor outlet temperature is clearly evidenced with increasing O/C ratio. The increase in the reactor outlet temperature was due to the greater exothermic nature of the reaction. The similar results obtained for the methane conversion, $H_2$+CO selectivity, $H_2$/CO ratio, and the compositions of the product gases between the systems in Table 2 (with the furnaces) and Table 5 (with the heat exchanger), revealed the possibility of increasing the energy efficiency of the ATR system.

## CONCLUSIONS

This study focused on the autothermal operation of a system in which an electric heater inside the reactor is used only to reach the ignition temperature and then the autothermal reaction is successfully maintained without any external heat source. The use of the heat exchanger at the back of the reactor showed the strong possibility of increasing the energy efficiency of the ATR system without any loss of performance. The values obtained, such as the methane conversion, $H_2$+CO selectivity, $H_2$/CO ratio, and the M factor, were adequate for the GTL process, while the question of the long-term stability of the system requires further study.

## ACKNOWLEDGMENTS

The authors would like to acknowledge the financial support of KEMCO and GTL Technology Development Consortium (Korea National Oil Corp., Daelim Industrial Co., LTD, Doosan Mecatec Co., LTD, Hyundai Engineering Co. LTD and SK Energy Co. LTD) under the Energy & Resources Technology Development Programs of the Ministry of Knowledge Economy, Republic of Korea.

## REFERENCES

1. R. Horn, K. A. Williams, N. J. Degenstein, A. Bitsch-Larsen, D. D. Nogare, S. A. Tupy and L. D. Schmidt, *J. of Catalysis*, **249**, 380 (2007).
2. A. P. E. Yorck, T. Xiao and M. L. H. Green, *Top. Catal.*, **22**, 345 (2003).
3. R. J. Farrauto, M. C. Hobson, T. Kennelly and E. M. Waterman, *Appl. Catal.*, **81**, 227 (1992).

4. S. Irandoust and B. Andersson, *Catal. Rev. Sci. Eng.*, **30**, 341 (1988).
5. V. R. Choudhary, V. H. Rane and A. M. Rajput, *Catal. Lett.*, **22**, 289 (1993).
6. Y. H. Hu and M. E. Ruckenstein, *J. of Catalysis*, **158**, 260 (1996).
7. T. L. Zhu and M. Flytzani-Stephanopoulos, *Appl. Catal. A*, **208**, 403 (2001).
8. A. T. Ashcroft, A. K. Cheethan, J. S. Foord, M. L. H. Green, C. P. Grey, A. J. Murrel and P. D. F. Vernon, *Nature*, **344**, 319 (1990).
9. A. K. Bhattacharya, J. A. Breach, S. Chand, D. K. Ghorai, A. Hartridge, J. Keary and K. K. Mallick, *Appl. Catal. A*, **80**, L1 (1992).
10. Y. Boucouvalas, Z. L. Zhang and X. E. Verykios, *Catal. Lett.*, **40**, 189 (1996).
11. S. Rabe, T.-B. Truong and F. Vogel, *Appl. Catal. A*, **318**, 54 (2007).
12. J. R. Rostrup-Nielson, *Catal. Today*, **63**, 159 (2000).
13. N. Mouaddib, C. Feumi-Jantou, E. Garbowski and M. Primet, *Appl. Catal. A*, **87**, 129 (1992).
14. P. M. Torniainen, X. Chu and L. D. Schmidt, *J. of Catalysis*, **146**, 1 (1994).
15. H. Jung, W. L. Yoon, H. Lee, J. S. Park, J. S. Shin, H. La and J. D. Lee, *J. Power Sources*, **124**, 76 (2003).